AJNR

Elastase-Induced Aneurysms in Rabbits: Effect of Postconstruction Geometry on Final Size

M. Onizuka, L. Miskolczi, M.J. Gounis, J. Seong, B.B. Lieber and A.K. Wakhloo

AJNR Am J Neuroradiol 2006, 27 (5) 1129-1131
http://www.ajnr.org/content/27/5/1129

ORIGINAL RESEARCH

M. Onizuka
L. Miskolczi
M.J. Gounis
J. Seong
B.B. Lieber
A.K. Wakhloo

Elastase-Induced Aneurysms in Rabbits: Effect of Postconstruction Geometry on Final Size

BACKGROUND AND PURPOSE: Elastase-induced aneurysms in rabbits have become an accepted model to study endovascular treatment. The size and shape of the resulting aneurysms may vary widely. Our goal was to predict the final aneurysm morphology on the basis of immediate postinduction geometry.

METHODS: Thirty New Zealand white rabbits were used. Aneurysms were created at the origin of the right common carotid artery (CCA). Intraluminal incubation of elastase was applied to the origin of CCA with proximal balloon occlusion of the artery. The aneurysms were allowed to mature for 3 weeks and evaluated by digital subtraction angiography. We retrospectively measured neck diameter, dome height, and aneurysm diameter, as well as the angle between the parent artery and the main axis of the aneurysm neck. We performed correlation analysis with immediate postinduction geometry.

RESULTS: The diameter of the origin of the CCA measured immediately after elastase incubation correlated positively to the mature aneurysm neck ($P < .01$). Moreover, the aneurysm neck both after the aneurysm creation and at 3-week follow-up had a positive correlation with the final dome height ($P < .05$). Finally, the dome height was related to the angle between the centerline of the innominate artery and axis of the aneurysm neck for dome diameter-to-neck ratio of <1.5 ($P < .05$).

CONCLUSION: These results indicate that neck width immediately after creation and the curvature of the parent artery are linked to the final aneurysm dimensions, and we may be able to predict the size of aneurysm on the day of creation.

An appropriate animal model of intracranial saccular aneurysms is needed for testing of a wide array of new devices. Canine and swine carotid sidewall aneurysms have been widely accepted by many investigators.[1] In 1999, Cloft et al introduced the elastase-induced aneurysm model in rabbits. It has been refined in the intervening years for preclinical testing of new endovascular devices.[2,3] These aneurysms, however, vary widely in shape. No published study is available on the stability of the aneurysm geometry after elastase induction. We retrospectively analyzed the geometry of the aneurysms by using digital subtraction angiography (DSA) at the time of induction and compared the data with the final aneurysm dimensions at 3 weeks. The purpose of the study was to predict the final aneurysm morphology on the basis of immediate postinduction geometry.

Methods

Aneurysm Construction

Thirty New Zealand white rabbits (3–4 kg body weight) were used for the study. Approval for the study was obtained from the animal care and use committee at our institution. Aneurysms were created as described elsewhere.[2] In brief, anesthesia was induced by intramuscular injection of 35 mg/kg ketamine and 5 mg/kg xalazine and continued by inhalation of 1.0%–1.5% isoflurane. The right common carotid artery (CCA) was isolated, and a 6F introducer sheath was placed in a retrograde fashion. The CCA was ligated distal to the sheath in a sterile fashion. A balloon catheter was positioned at the right CCA origin, and a microcatheter was advanced side by side with the shaft of the balloon catheter. To avoid any damage to the balloon catheter, the microcatheter and the nondetachable silicone balloon catheter (Endeavor, Target Therapeutics, Fremont, Calif) were placed through the same 8F guiding catheter. The tip of the guiding catheter was introduced into the sheath just beyond the diaphragm. The balloon catheter positioned at the CCA origin was inflated with just enough iodinated contrast medium (Omnipaque 300, Nycomed, Princeton, NJ) to achieve flow arrest in the CCA. Subsequently, the position of the microcatheter tip was verified by injection of approximately 1 mL of contrast. After flushing the microcatheter with isotonic saline, a solution containing 50 U of porcine pancreatic elastase (5.23 U/mg, 40.1 mg/mL; Worthington Biochemical Corporation, Lakewood, NJ) mixed with saline and iodinated contrast medium was incubated in the dead space of the CCA, between the inflated balloon and the ligature, for approximately 15 minutes. After incubation, the elastase solution was removed via the sheath by aspiration, and the balloon was deflated. Contrast injection through the sheath into the brachiocephalic trunk displayed the washout of the contrast at the CCA origin and verified initial dilation. We measured the diameter of the origin CCA on the DSA images immediately after elastase incubation by using a metal washer as a calibration marker (Fig 1). Both the balloon catheter and microcatheter were removed, the sheath was withdrawn, and carotid artery ligature was secured. Finally, the wound was closed in multiple layers with 3–0 Vicryl. The procedure lasted for approximately 1 hour.

Follow-Up Angiography

Aneurysms were allowed to mature at least 21 days. Subsequently, each animal underwent follow-up studies with selective arterial angiograms through a right femoral artery approach. After a cut-down of the right femoral artery and placement of a 4F sheath, catheterization was accomplished with a 4F guiding catheter. The tip of a 4F

Received July 29, 2005; accepted after revision October 5.

From the Department of Neurosurgery (M.O.), Fukuoka University Chikushi Hospital, Fukuoka, Japan; Center for Neuroendovascular Surgery and Stroke Research (L.M., B.B.L.), Department of Radiology, Miller School of Medicine, and Department of Biomedical Engineering (J.S., B.B.L.), University of Miami, Miami, Fla; and the Division of Neuroimaging and Intervention (M.J.G., A.K.W.), Department of Radiology, University of Massachusetts Medical School, Worcester, Mass.

Address correspondence to Ajay K. Wakhloo MD, PhD, Division Neuroimaging and Intervention, Department of Radiology, University of Massachusetts Medical School, 55 Lake Avenue North, Worcester, MA 01655.

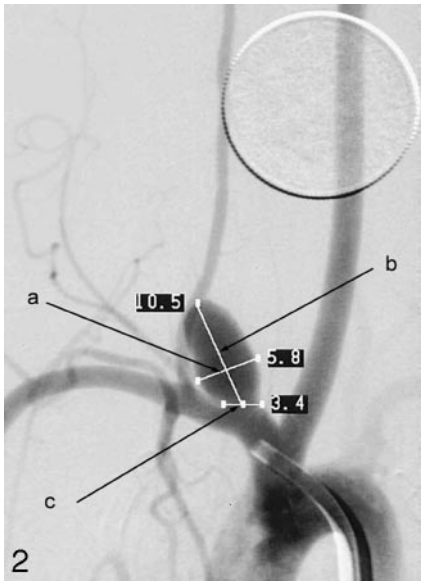

Fig 1. Angiogram shows the right common carotid artery after elastase incubation. The arrow indicates the proximal origin of the common carotid artery.

Fig 2. Three-week follow-up angiogram after creation of the aneurysm. a, dome diameter, b, dome height, c, neck width.

guiding catheter was placed in the innominate artery, and DSA angiograms were obtained in a plane that clearly depicted the aneurysm neck. We then measured the geometric attributes of the created aneurysm such as dome height, dome diameter, and neck width (Fig 2).

Image Analysis

Angiograms of elastase-induced aneurysms in rabbits were acquired by using a DSA angiography unit (Siemens Angiostar, Forchheim, Germany). We used an imaging software (Merge eFilm 1.5, Milwaukee, Wis) to convert the DICOM images generated by the angiography unit into JPEG format and transferred to a personal computer for further analysis. The grayscale JPEG images of the aneurysms and vasculature in their immediate vicinity were then converted to binary images by threshold filtering by using Adobe Photoshop 5.0 (Adobe Systems, San Jose, Calif) and Scion Image (shareware NIH image-processing program [http://www.scioncorp.com]) (Fig 3*A*). Values greater than the threshold were considered noise and set to white, whereas values less than the threshold were set to black. The centerlines of the vasculature in the binary images were obtained by a parallel symmetric thinning operation,[4,5] and the outline of the bifurcation was found by an edge-detection operation in MATLAB (MathWorks, Natick, Mass).[6] The high-performance thinning algorithm executes fully symmetric erosion to obtain the centerline (Fig 3*B*). Once thinning operation was completed in each image, a polynomial function was fit to the centerline of aneurysms and parent arteries, and the angles between the parent arteries to aneurysm neck were calculated from the tangents to the curves at their intersections (Fig 3*C, -D*). Additional information on angle calculations is detailed in the report of Seong et al.[7]

Statistical Evaluations

A regression analysis was performed by using Statview (SAS, Cary, NC), and the Pearson correlation coefficient (r) was calculated for the relationship between the angle between the aneurysm and parent artery, dome height, neck and dome width.

Results

On the basis of the ratio of dome diameter-to-neck width (D/N) in 30 aneurysms (Table 1) we divided the constructed aneurysms into 3 groups. The ratio D/N ranged from 0.59 to 3.78 with a mean of 1.47 ± 0.6 mm (mean ± SD). Eighteen aneurysms were found to have a D/N <1.5, and the remaining 12 aneurysms showed a D/N >1.5. Sixty percent of the aneurysm had a wide neck (D/N <1.5). Immediately after elastase incubation the diameter of the origin CCA measured 2.9 ± 0.8 mm (mean ± SD; range, 1.25–5.07 mm) and correlated positively with the aneurysm neck at 3-week follow up ($y = 0.715x + 0.882$; $r^2 = 0.328$; $P < .01$). Moreover, the aneurysm neck both immediately after creation and at 3-week follow-up showed a positive correlation with the final dome height ($y = 1.349x + 5.96$; $r^2 = 0.164$; $P < .05$). Finally, the dome height was found to be proportional to the angle between the innominate artery and the aneurysm neck for D/N <1.5 ($y = 0.132x - 7.51$, $r^2 = 0.321$; $P < .05$).

Summary of dimensions

Location	Average Value	Range
Angle (°)	124.6 ± 13	96–148
Dome height (mm)	10 ± 2.8	4.7–14.7
Dome width (mm)	4.2 ± 1.2	1.6–6.7
Neck width (mm)	3 ± 1.5	0.9–8.7

Note:—Angle indicates the angle between innominate artery and aneurysm neck. Average values are mean ± SD.

Discussion

In our study the geometric data of experimental aneurysms in rabbits were similar to those reported previously by Short et al[8] and comparable to those found in humans. In their series, Short et al measured a width of aneurysmal pouch of 4.1 ± 1.2 mm (mean ± SD; range, 2.5–7.1 mm). The aneurysm height ranged from 3.0 to 15.6 mm (mean, 8.8 ± 2.6 mm). The geometry of the parent vessel in relation to the orientation of the aneurysm plays a significant role in determining the final shape and size of the aneurysm. This may be related to local hemodynamics in and around the aneurysm.[9] Because the angle of approach between the aneurysm neck axis and the incoming flow gets smaller, it is more likely that flow impingement will occur in the vicinity of the aneurysm distal neck or inside the aneurysm itself. Therefore, the washout of blood from the aneurysm dome with each heartbeat will be more

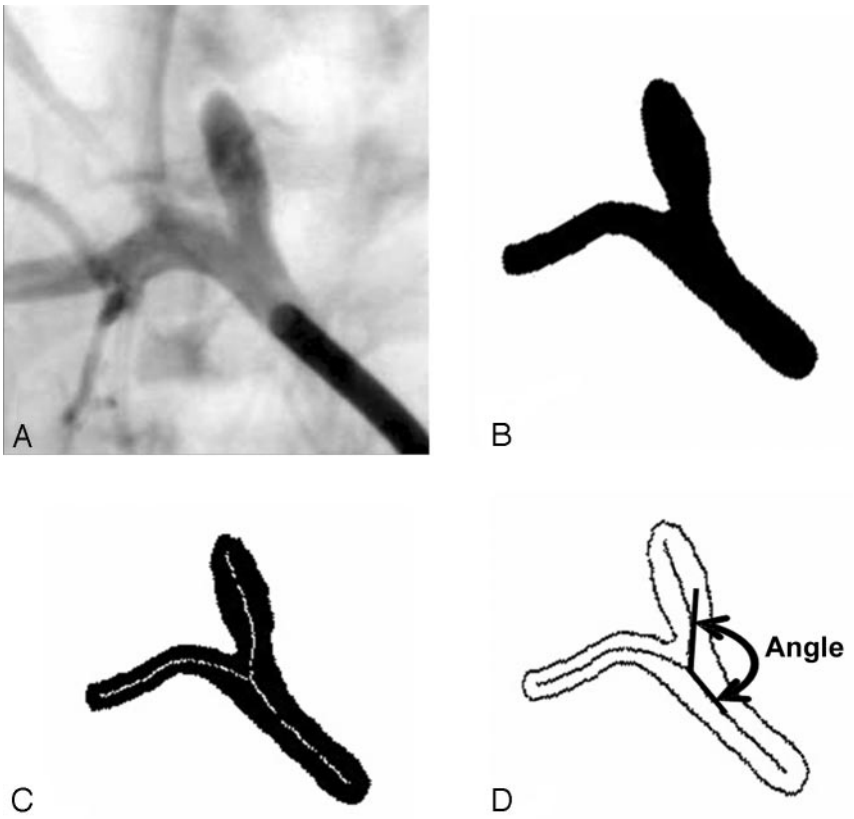

Fig 3. Illustration shows the angle between innominate artery and the aneurysm. *A,* Original nonsubtracted angiogram. *B,* Skeleton image. *C,* Skeleton image with center line. *D,* Angle between the parent artery and the aneurysm neck

rigorous. Consequently, a larger aneurysm volume will remain viable during the remodeling period. As the radius of curvature of the parent vessel decreases, flow impingement on the distal neck leads also to elevations in wall shear stress at that region and, as a result, the impact zone at the distal neck of the aneurysm increases, which can lead to formation of a wider-neck aneurysm.

When experimental studies for testing various devices are designed by using canine carotid sidewall aneurysms, the aneurysm size is controlled by the size of the vein-pouch used. Treatment of the aneurysm and testing of devices can be performed immediately after aneurysm creation; however, the biologic response to devices or implants and their similarity to the biologic response in humans have been criticized. The elastase-induced aneurysm in rabbit represents a superior model for the investigation of biologic response to bioimplant. The size of rabbit arteries harboring the experimental aneurysm is very similar to the size of human intracranial vessels and macroscopically closely resembles bifurcation aneurysms found in humans.[8] A maturation period of 2–3 weeks, however, is required before the final morphology of the created model can be assessed.[10,11] If one could predict the final morphology of the constructed aneurysm immediately after creation, substantial savings in time, cost, and effort could result. Among the 30 aneurysms we created, 60% were classified as wide necked. The final aneurysm morphology could have been predicted on the basis of immediate postinduction geometry.

Limitations of this study include the relatively sparse data base on which the geometric features were evaluated. Although we attempted to obtain angiographic projections that were parallel to the aneurysm/parent artery plane, some small variations among the projections is unavoidable, because the arterial structures of interest do not necessarily lie in a flat plane. Therefore, it is possible that differences in the projections may account for small differences in aneurysm sizes. Another limitation of this investigation is the lack of histologic findings to compare with the radiologic results. We are now pursuing improvements to this aneurysm model to better understand the relation between the hemodynamic forces involved in vascular remodeling and aneurysm growth.

Conclusions

It appears that the geometric relationship between the major aneurysm axis and the parent artery in the elastase-induced aneurysm in rabbits immediately after construction play a significant role in determining the local hemodynamics and, consequently, the final aneurysmal architecture. Histologic analysis is needed to correlate histologic findings with the local hemodynamics and further substantiate the angiographic results.

Acknowledgments

This work was supported in part by the National Institutes of Health under grant R01 NS045753–01A1. We are grateful to Ms. Lilliana Cesar for her superb care of the animals and her help during the experimental procedures.

References

1. Kallmes DF, Altes TA, Vincent DA, et al. **Experimental side-wall aneurysms: a natural history study.** *Neuroradiology* 1999;41:338–41
2. Cloft HJ, Altes TA, Marx WF, et al. **Endovascular creation of an in vivo bifurcation aneurysm model in rabbits.** *Radiology* 1999;213:223–28
3. Miskolczi L, Guterman LR, Flaherty JD, et al. **Saccular aneurysm induction by elastase digestion of the arterial wall: a new animal model.** *Neurosurgery* 1998; 43:595–600
4. Bourbakis N, Steffensen N, Saha B. **Design of an array processor for parallel skeletonization of images.** *IEEE Trans Circuits Syst II: Analog Digital Signal Processing* 1997;44:284–98
5. Lam L, Lee SW, Suen CY. **Thinning methodologies-A comprehensive survey.** *IEEE Trans Pattern Anal Machine Intelligence* 1992;14:869–85
6. Gonzalez, RC, Woods RE. *Digital image processing.* Reading, MA: Addison-Wesley;1992:518–60
7. Seong J, Lieber BB, Wakhloo AK. **Morphological age-dependent development of the human carotid bifurcation.** *J Biomech* 2005;38:453–65
8. Short JG, Fujiwara NH, Marx WF, et al. **Elastase-induced saccular aneurysms in rabbits: comparison of geometric features with those of human aneurysms.** *AJNR Am J Neuroradiol* 2001;22:1833–37
9. Seong J, Lieber BB, Wakhloo AK. **Compliant silicone elastomer models of elastase-induced aneurysms in the rabbit: model construction and hemodynamics.** Presented at: ASME International Mechanical Engineering Congress & Exposition Anaheim, CA, November 13–19, 2004
10. Fujiwara NH, Cloft HJ, Marx WF, et al. **Serial angiography in an elastase-induced aneurysm model in rabbits: evidence for progressive aneurysm enlargement after creation.** *AJNR Am J Neuroradiol* 2001;22:698–703
11. Kallmes DF, Fujiwara NH, Berr SS, et al. **Elastase-induced saccular aneurysms in rabbits: a dose-escalation study.** *AJNR Am J Neuroradiol* 2002;23:295–98